Substrate orientation dependence of enhanced epitaxial regrowth of silicon

K. T. Ho, I. Suni,[a] and M-A. Nicolet
California Institute of Technology, Pasadena, California 91125

(Received 25 August 1983; accepted for publication 19 October 1983)

This work extends the study of dopant-enhanced epitaxial regrowth rate of amorphized Si from the ⟨100⟩ to the ⟨110⟩ and ⟨111⟩ orientations of Si. Boron and phosphorus dopants are considered. The annealing temperatures are 500 and 550 °C. Phosphorus enhances the growth rates in all three orientations by a constant factor of 8.1 ± 0.9. Boron produces a higher enhancement factor of 12.2 ± 1.2, except in the case of ⟨100⟩. Implications of the results on various growth models are considered. The crystalline quality of regrown ⟨111⟩ layers is improved in the doped samples.

INTRODUCTION

Regrowth of Si by solid phase epitaxy (SPE) is a part of most device fabrication processes that use high dose implantation doping. Another recent example is the preamorphization of Si by self-implantation to control the projected range of boron implantation in a shallow junction.[1] Dopant enhanced SPE regrowth is thus gaining technological significance in addition to its scientific interest.

The original work on dopant-enhanced regrowth of Si was done by Csepregi *et al.*,[2] who demonstrated that impurities such as B, P, and As can significantly accelerate the regrowth rates of amorphized Si on ⟨100⟩ substrates. Subsequently, Nishi *et al.*[3] looked at As-doped amorphized layers on ⟨100⟩, ⟨110⟩, and ⟨111⟩ substrates with detailed analysis of electrical activation during regrowth. It was shown that dopants become partially or totally activated as they get incorporated into the advancing recrystallized region. Recently, Suni *et al.*[4] and Lietoila *et al.*[5] demonstrated that the enhancement is an electrically activated effect by showing that *p*-type and *n*-type dopants together mutually compensate and do not produce an enhanced growth rate. Explanations of the enhancement in terms of electronic processes are given by Suni *et al.*[6] and Williams *et al.*[7]

These previous works have studied SPE regrowth principally on ⟨100⟩ Si substrates. The current work aims at a systematic survey of the enhanced regrowth on other substrate orientations, namely ⟨111⟩ and ⟨110⟩, in addition to ⟨100⟩ which was also included for reference.

Substrate orientation dependence of SPE was first reported by Csepregi *et al.*[8] on undoped Si. The regrowth velocities of each orientation differ and decrease in the order $v_{100} > v_{110} > v_{111}$. A model based on geometrical arguments was used to explain this dependence. A recent atomistic model proposed by Narayan[9] correctly predicts the relative regrowth rates of the different orientations.

This work incorporates the above two subjects that have been separately studied before, namely, enhanced regrowth and substrate orientation dependence of Si SPE regrowth. Previous studies have shown that, for ⟨100⟩ Si, B-doped samples grow faster than P-doped ones. This work looks at such dopant dependences for B and P implantations.

EXPERIMENTAL METHODS

The starting wafers were *p*-type ⟨100⟩ with resistivity of 1.5–2.5 Ω cm ($\sim 10^{16}$ B/cm^3), *p*-type ⟨110⟩ with resistivity of 0.017 Ω cm ($\sim 5 \times 10^{18}$ B/cm^3), and *n*-type ⟨111⟩ with resistivity of 0.005–0.020 Ω cm ($\sim 1.5 \times 10^{18}$–1.5×10^{19} Sb/cm^3). The principal axis of ⟨111⟩ wafers was about 3° off the sample normal, while the ⟨110⟩ and ⟨100⟩ axes coincided with the respective sample normal. The wafers were cleaned and diced for one of the three sequences of multiple implantations at liquid nitrogen temperature. The sequences were (i) ^{28}Si only (denoted as I), (ii) ^{28}Si, ^{11}B (denoted as B), (iii) ^{28}Si, ^{31}P (denoted as P). Si implantation preceeded B and P implantations to ensure complete amorphization. Sample normals were tilted 8° from the incident ion beam to avoid channeling effects.

The dose and energy combination was selected such as to produce an extended region, approximately 6000 Å deep, of constant dopant concentration. Range tables by Smith[10] have been used to calculate the final dopant distributions, shown in Figs. 4 and 5. The implantation schedules are provided in Table I.

The plateau of the B and P profiles corresponds to a concentration of about 2×10^{20}/cm^3, well exceeding the de-

TABLE I. Implantation schedules for silicon, boron, and phosphorus. All implantations were performed at LN_2 temperature, with the sample normal tilted by 8° from the beam to minimize channeling effects.

Dopant	Ion species	Dose (10^{15} atom/cm^2)	Energy (keV)
^{28}Si	Si^+	1	60
	Si^+	2	140
	Si^+	5	300
^{11}B	B^+	2.5	60
	B^+	3.4	115
	B^+	4.1	200
^{31}P	P_2^+	1.4	180
	P_2^+	2.5	320
	P^+	6.7	320

[a] Permanent Address: Semiconductor Laboratory, Technical Research Centre of Finland, Otakaari 5A, SF 02150, Espoo 15, Finland.

 0021-8979/84/161207-06$02.40

generate doping level, but still below the solid solubility limit of B and P in Si in the temperature range used for regrowth.[11] Given the low diffusion coefficients of B and P in Si,[11] no redistribution of the implanted dopants is expected during regrowth. Recent studies of Sadana *et al.*[12] also demonstrated the lack of redistribution of P in regrown amorphized Si. Annealing was done in a vacuum furnace at temperatures of 500 °C or 550 °C. Thicknesses of the amorphous layers are derived from channeling spectra obtained using 1.5-MeV $^4He^+$ ions.

RESULTS

Dopant dependence for each substrate orientation

⟨100⟩ Si (Fig. 1)

Our regrowth rate for intrinsic Si is approximately 11.6 Å/min which is slightly higher than the value reported by Csepregi *et al.*[8] at 500 °C. In the P-implanted sample, the regrowth rate reaches a constant level of 92.4 Å/min in the uniformly doped region. The regrowth is even faster in the B-implanted sample where the measured growth rate is approximately 241.0 Å/min. These rates are in fairly good agreement with previously reported values. They are summarized in Table II.

There is an initial fast growth in the intrinsic sample which may be related to an incompletely amorphized region due to the trailing edge of the implanted Si profile. In the experiments of Csepregi *et al.*, a low temperature (~450 °C) preannealing was performed to eliminate the damaged region.[13] No initial fast growth is reported in those results.

⟨110⟩ Si (Fig. 2)

Regrowth enhancement by B and P doping is observed for the ⟨110⟩ orientation as well, as shown in Fig. 2. Our intrinsic growth rate is 6.3 Å/min, faster than that of Csepregi *et al.*[8] (shown in dashed line). The P-implanted sample regrows at a constant rate of 45.1 Å/min in the uniformly doped region, while the B-implanted sample regrows at a faster rate of 84 Å/min.

TABLE II. Regrowth rates at 500 °C (Å/min).

	This work	Csepregi *et al.* (Ref. 2)	Suni *et al.* (Ref. 4)	Nishi *et al.* (Ref. 3)	Lietoila[b] *et al.* (Ref. 5)
Doping level (10^{20}/cm^3)	2	2–3	4	2 max	2
I⟨100⟩	11.6	10.0	7.0		6.93
⟨110⟩	6.3	3.5			
⟨111⟩		1.5[a]			
B⟨100⟩	241	200	177		
⟨110⟩	84				
⟨111⟩	18				
P⟨100⟩	92.4	61	88		52
⟨110⟩	45.1				
⟨111⟩					
As⟨100⟩		55	39.4	40	
⟨110⟩				11	
⟨111⟩				1.3	

[a] Extrapolated from Arrhenius plot.
[b] Annealed at 503 °C.

⟨111⟩ Si (Fig. 3)

Because the intrinsic regrowth rate of ⟨111⟩ Si at 500 °C is impractically slow (~1.5 Å/min), this orientation was also studied at 550 °C, so that an intrinsic growth curve can be obtained for comparison. The results for 500 °C annealing are included in Figs. 4 and 5.

The intrinsic growth curve shows the same break as observed by Csepregi *et al.*,[8] but at a larger regrown thick-

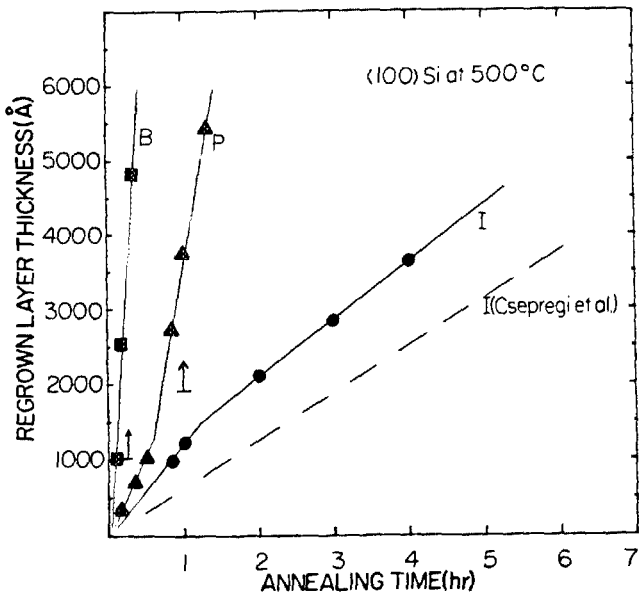

FIG. 1. Regrowth curves of doped and intrinsic ⟨100⟩ Si, at an annealing temperature of 500 °C. The dashed line is taken from Csepregi *et al.* Arrows next to the B and P growth curves indicate beginnings of constant concentration regions.

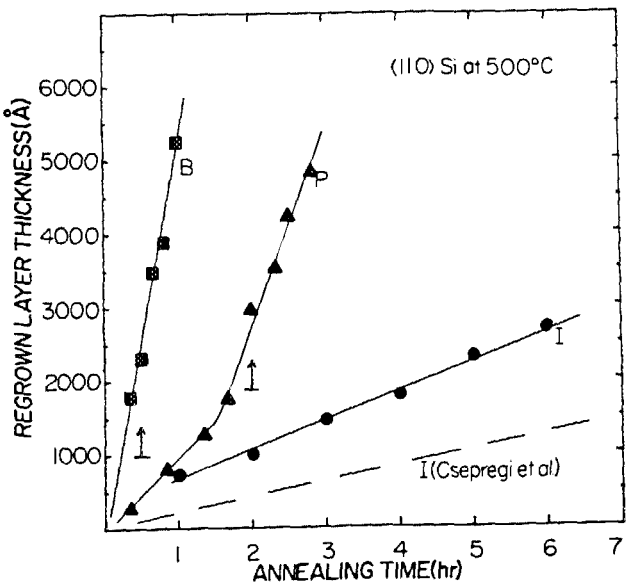

FIG. 2. Regrowth curves of ⟨110⟩ Si at 500 °C. The dashed line is taken from Csepregi *et al.*

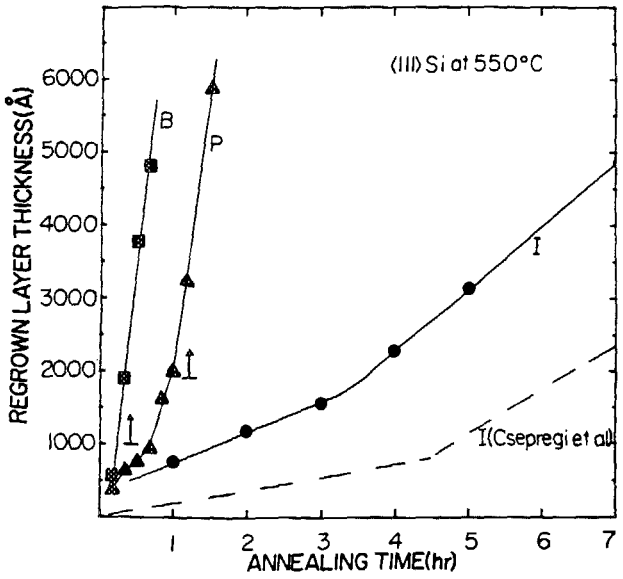

FIG. 3. Regrowth curves of ⟨111⟩ Si at an annealing temperature of 550 °C. The slow and fast growth regions are similar to the results of Csepregi *et al.* (dashed line).

ness. At 550 °C the slow growth progresses at a rate of 6.6 Å/min, and the fast growth, at a rate of 14.4 Å/min, both slightly higher than the corresponding rates reported by Csepregi *et al.* The P-implanted sample reaches a constant growth rate of 129.0 Å/min, and the B-implanted sample, a rate of 154.7 Å/min, in their respective uniformly doped regions.

Orientation dependence with fixed dopant type

Figures 4 and 5 show that the growth rates for different orientations are related in the same way in doped samples as

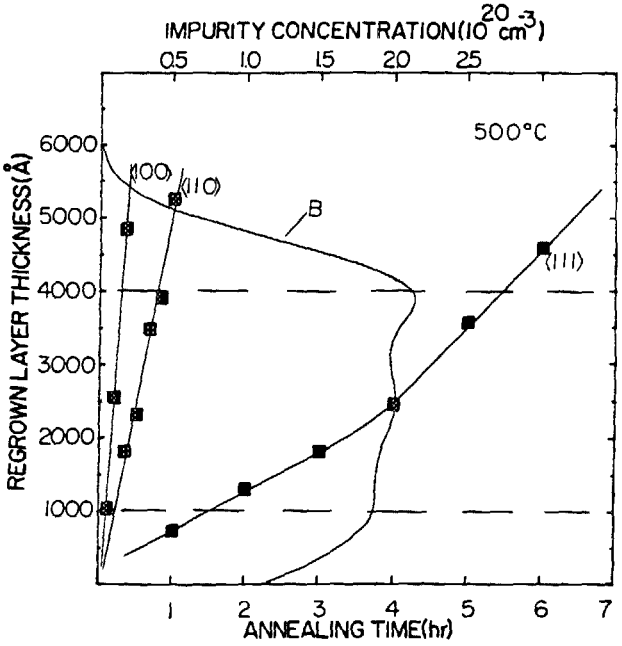

FIG. 4. Substrate orientation dependence of regrowth rate for B-implanted Si at 500 °C annealing. Growth velocities decrease in the order $v_{100} > v_{110} > v_{111}$ similar to intrinsic samples. The calculated concentration profile of the implanted boron is also plotted. The area between dash lines is taken at the constant concentration region.

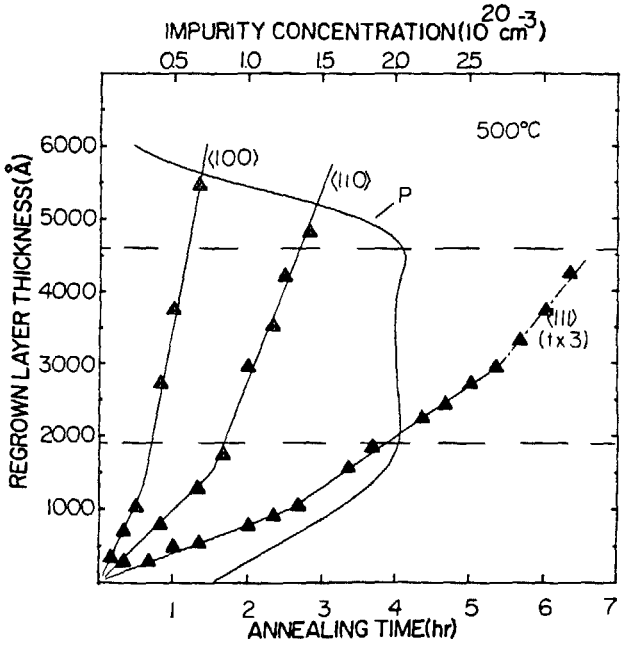

FIG. 5. Phosphorus implanted samples show the same substrate orientation dependence as the B-implanted and intrinsic samples. The annealing temperature is 500 °C. The calculated P concentration profile is also plotted. Due to the slow regrowth rate of the ⟨111⟩ sample, the time scale is contracted by a factor of 3 to fit this growth curve into the figure. The P⟨111⟩ growth curve ends in a dash-dot line to indicate that the amorphous-crystalline interface has become very nonuniform.

they are in the intrinsic case, namely, $v_{100} > v_{110} > v_{111}$. At 500 °C annealing temperature, the B⟨111⟩ and P⟨111⟩ samples appear to have two regrowth rates in the constant concentration region. Phosphorus-doped samples become very nonuniform at the amorphous-crystalline interface after prolonged annealing. The end section of the P⟨111⟩ growth curve therefore has an uncertain meaning and is left as a dash-dot line.

Additional observations

In the six month period in which this experiment was carried out, scattering of data points did not exceed 17% in the worst case of B⟨110⟩. The growth curve for each doped sample (except the ⟨111⟩ samples at 500 °C) was obtained from a number of specimens annealed only once. Each intrinsic growth curve (and the doped ⟨111⟩ samples at 500 °C) includes data points obtained by sequentially annealing of a few specimens. Reproducibility has been checked for some growth curves and good agreement was found.

The quality of SPE on ⟨111⟩ substrates is plagued by twin formations leading to bilinear growth and high channeling yields.[14,15] This is explained by Drosd *et al.* and Narayan to come from the requirement of 3 atoms to complete the first sixfold ring of a recrystallizing plane in ⟨111⟩ direction, as compared to 2 atoms required for ⟨110⟩ and 1 atom for ⟨100⟩ plane. The high chance of a twin formation is due to the high probability of the 3 atoms nucleating in the wrong configuration. We may assume that twin nucleations occur at a certain rate at the amorphous-crystalline interface, in competition with epitaxial regrowth. Since the growth front advances at a faster velocity in a doped sample, twin nuclea-

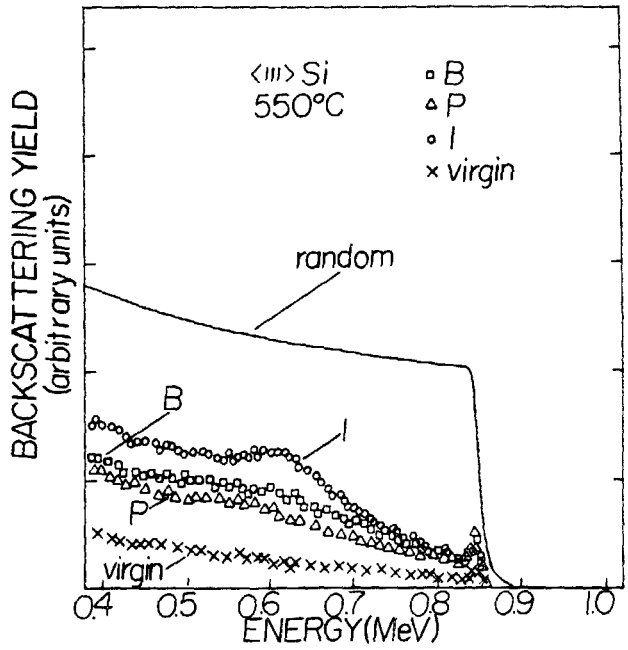

FIG. 6. Channeling spectra of fully regrown boron, phosphorus, and Si implanted ⟨111⟩ samples, plotted against the channeled and random spectrum of an unimplanted sample. Implanted dopants reduce channeling yields as compared to the spectrum of the intrinsic sample, indicating an improvement of crystalline quality. The implanted samples were regrown at 550 °C. The annealing times were 4, 4, and 8 h for B-doped, P-doped, and intrinsic samples, respectively.

tion density per regrown thickness is expected to be correspondingly reduced. Faster regrowth therefore should improve the crystalline quality. This is verified by channeling spectra of the completely regrown samples shown in Fig. 6, in which B- and P- implanted samples demonstrate an overall reduction in yield. All regrown samples show a faster climb in yield, as compared to the virgin sample, from the surface to the original amorphous-crystalline interface, indicating dechanneling due to residual defects. This means that the crystalline quality is still severely degraded with respect to the virgin sample.

DISCUSSION

Various models have been proposed for the mechanism of SPE regrowth. Csepregi *et al.*[8] assume that an atom can be attached to the crystalline phase only at sites where at least two nearest neighboring atoms at the interface are already in crystalline positions. Geometrical inspection then indicates that ⟨111⟩ plane is the slowest growing direction, giving rise to ⟨111⟩ facets.

In the model by Spaepen *et al.*,[16] attachment of each new atom to a crystalline site involves breaking one bond to rearrange the five- or sevenfold rings characteristic of the amorphous phase to a sixfold ring of the diamond crystalline phase.[17] This broken bond runs along a [110] ledge reconstructing crystalline sites in its path. Spaepen suggests that the bond breaking process is the controlling mechanism for SPE regrowth.

In the work by Drosd and Washburn[18] and that by Narayan,[9] two similar and congruent models of SPE regrowth are presented. Each involves nucleation of atomic steps on a flat crystalline plane at the amorphous-crystalline interface. The step then laterally spreads into a new crystalline layer. Drosd *et al.* attribute the SPE regrowth activation energy to the reorientation of a small group of atoms in the amorphous material at the interface. Narayan takes a very different view and proposes that the activation energy is that for the self diffusion in amorphous Si near the interface. Since Narayan argues that only migration energy is involved in this type of diffusion, this interpretation does not relate the activation energy to the formation of point defects.

It was pointed out by Csepregi *et al.*[19] that the activation energy of the SPE regrowth for both Si and Ge lies within the range quoted for the formation energy of vacancies in the respective materials. Based on this correlation, Suni *et al.*[6] suggested that vacancies at the amorphous-crystalline interface control and accelerate the bond breaking process which necessarily precedes atomic rearrangement during recrystallization. The same authors estimated the reduction of regrowth activation energy by considering the energy levels of charged vacancies and the shift of Fermi level induced by dopants. A qualitative agreement with experimental data was found.

Thus far, the controlling mechanism of SPE regrowth has been variously attributed to:

(1) Vacancy formation (Csepregi *et al.*,[19] Suni *et al.*[6]);

(2) Bond breaking/propagation of loose bonds (Spaepen *et al.*[16]);

(3) Self-diffusion in amorphous Si (Narayan[9]).

In order to shed light on this subject, a compilation of data by various authors is presented in Table II to illuminate any consistencies and patterns which may emerge from the many research efforts. Growth rates are seen to vary by up to 44% in the worst case. However, it should be noted that in the work done by Csepregi *et al.*[2] and Nishi *et al.*,[3] the implantations did not produce a region of constant doping level. Although Csepregi *et al.* made the observation that the growth velocity becomes approximately constant for P concentration between 2 and $3\times10^{20}/\text{cm}^3$, it is not clear how reliably growth rates can be measured in such situations. Other factors leading to discrepancies are offsets in temperature and impurities incorporated during implantation, such as nitrogen and carbon, which are known to slow down the growth velocities.[20] The ⟨100⟩ orientation of each dopant type is studied most extensively, and may serve as the standard in making cross references.

The enhancement effect can be measured in terms of the enhancement factor defined as the ratio of the rates of the doped samples to the intrinsic sample of the same orientation. In ⟨100⟩ Si the enhancement factor is 8.0 for P-implanted samples, and 20.8 for B-implanted samples. In ⟨110⟩ Si, P produces an enhancement factor of 7.2, and B, a factor of 13.3.

The ⟨111⟩ results are complicated by a bilinear growth characteristic of the intrinsic samples, with the final fast growth region dominated by formation of large twin planes inclined to the surface.[8] This makes a quantitative comparison with doped samples difficult. However, the faster growth rate can be interpreted as the growth rate of ⟨111⟩

TABLE III. Regrowth rates and enhancement factors: I, P, and B doped ⟨100⟩, ⟨110⟩, and ⟨111⟩ silicon.

		I		B		P	
		Growth rate	Enhancement factor	Growth rate	Enhancement factor	Growth rate	Enhancement factor
500 °C	⟨100⟩	11.6	...	241	20.8	92.4	8.0
	⟨110⟩	6.3	...	84	13.3	45.1	7.2
	⟨111⟩	1.5[a]		18		7.6	
		0.4	...	8.6	...	3.7	...
550 °C	⟨111⟩	14.4	...	154.7	11.0	129	9.0

[a] Extrapolated from Arrhenius plot of Csepregi *et al.* (from Ref. 8).

oriented wafers averaged over the twined and perfectly epitaxial sections on the growth front. Since a predominant part of the amorphized region regrows at the fast rate, it is more practical to emphasize this rate. We therefore calculate the ⟨111⟩ enhancement factor according to the faster intrinsic rate as is done by Csepregi *et al.*[2] At 550 °C, the doped samples show only one growth rate in the constant concentration region, giving an enhancement factor of 9.0 for P-implanted samples, and 11.0 for B-implanted samples. At 500 °C, both P- and B-implanted samples show two growth rates in the constant concentration region. Whether twin formations are responsible here for the different rates cannot be determined without TEM studies. Both slow and faster growth rates of these samples are included in Table III. Enhancement factors cannot be meaningfully defined in this case.

Table III provides an overview of the current experimental results. The enhancement factors due to P range from 7.2 to 9.0, which may be considered to be a constant value of 8.1 ± 0.9. The enhancement factor due to boron is 12.2 ± 1.2. However, this value excludes the exceptionally high value of 20.8 for B⟨100⟩.

Based on this interpretation of data, it can be stated that the primary mechanism responsible for regrowth enhancement is independent of the crystal orientation. The exceptionally high value for B⟨100⟩ then indicates that an additional mechanism for enhancement is taking effect in this sample configuration.

The model of Suni *et al.*[6] which explains the enhancement by a reduction in activation energy due to dopant induced charged vacancies, would be in agreement with our findings. This is because in this model, all substrate related geometrical factors are included in the preexponential term, which is unaffected after doping. Narayan's model[9] which described an enhanced self-diffusion in amorphous Si is also consistent with the orientation independence. The model of Spaepen *et al.*[16] looks at bond breaking and loose bond propagation. The interfacial conditions in which these processes occur differ for each orientation. Whether the enhancement according to this model should be constant is not clear. (It is also unclear that Spaepen *et al.* wanted to apply the model to other than the ⟨111⟩ orientation).

Our ⟨111⟩ wafers have an original doping level within one order of magnitude of the implanted value. The question is whether this relatively high background enhances the regrowth. In the works of Csepregi *et al.*[2] and Suni *et al.*,[6] various growth curves are superimposed on corresponding dopant profiles. We determine from their figures that any enhancement effect due to this background doping level is negligible.

CONCLUSION

Dopant enhanced SPE regrowth has been demonstrated to take place for ⟨111⟩ and ⟨110⟩, as well as ⟨100⟩ oriented Si, at both 500 and 550 °C. Samples implanted with P exhibit an enhancement factor of 8.1 ± 0.9; while B-implanted samples have a factor of 12.2 ± 1.2, except in case of B⟨100⟩, which has a high value of 20.8. We find consistency with previously reported results that B is more effective than P in accelerating the SPE regrowth velocity. A constant enhancement factor for different orientations is, by itself, not sufficient to distinguish whether the primary controlling mechanism of regrowth is due to vacancy formation, bond breaking and propagation, or self-diffusion in amorphous Si, as proposed by various authors. The faster regrowth induced by B and P improves crystalline quality in the regrown layer by partially suppressing competing twin formations.

ACKNOWLEDGMENTS

The authors would like to thank Dr. S. S. Lau (University of California, San Diego) for valuable discussions. The implantation part of this study was financially supported by the U. S. Department of Energy through an agreement with the National Aeronautics and Space Administration and monitored by the Jet Propulsion Laboratory, California Institute of Technology (D. Burger).

[1] T. M. Liu and W. G. Oldham, Extended abstract No. 406, ECS spring meeting (1983); to be published in J. Electrochem. Soc.
[2] L. Csepregi, E. F. Kennedy, T. J. Gallagher, and J. W. Mayer, J. Appl. Phys. **48**, 4234 (1977).
[3] H. Nishi, T. Sakurai, and T. Furuya, J. Electrochem. Soc. **125**, 461 (1978).
[4] I. Suni, G. Göltz, M. G. Grimaldi, and M-A. Nicolet, Appl. Phys. Lett. **40**, 269 (1982).
[5] A. Lietoila, A. Wakita, T. W. Sigmon, and J. F. Gibbons, J. Appl. Phys. **53**, 4399 (1982).
[6] I. Suni, G. Göltz and M-A. Nicolet, Thin Solid Films **93**, 171 (1982).
[7] J. S. Williams and K. T. Short, Proceedings of the International Conference on Ion Beam Modification of Materials (IBMM-82), Grenoble, France, September (1982), Vol. 10, p. 123.
[8] L. Csepregi, E. F. Kennedy, and J. W. Mayer, J. Appl. Phys. **49**, 3906 (1978).
[9] J. Narayan, J. Appl. Phys. **53**, 8607 (1982).
[10] B. Smith, *Ion Implantation Range Data For Silicon and Germanium Device Technologies* (Research Studies Press, Forest Grove, Oregon, 1977).

[11]S. M. Sze, *Physics of Semiconductor Devices*, 2nd edition (Wiley-Interscience, New York, 1981).
[12]D. K. Sadana, J. Washburn, and C. W. Magee, J. Appl. Phys. **54**, 3479 (1983).
[13]S. S. Lau (private communication).
[14]L. Csepregi, J. W. Mayer, and T. W. Sigmon, Appl. Phys. Lett. **29**, 92 (1976).
[15]G. Foti, L. Csepregi, E. Kennedy, P. Pronko, and J. W. Mayer, Phys. Lett. **64A**, 265 (1977).
[16]F. Spaepen and D. Turnbull, in *Laser-Solid Interactions and Laser Processing*, edited by S. D. Ferris, H. J. Leamy, and J. M. Poate (American Institute of Physics, New York, 1979), p. 73.
[17]F. Spaepen, Acta Metall. **26**, 1167 (1978).
[18]R. Drosd and J. Washburn, J. Appl. Phys. **53**, 397 (1982).
[19]L. Csepregi, R. Küllen, J. W. Mayer, and T. W. Sigmon, Solid State Commun. **21**, 1019 (1977).
[20]E. F. Kennedy, L. Csepregi, J. W. Mayer, and T. W. Sigmon, J. Appl. Phys. **48**, 4241 (1977).